IEEE Photonics Journal
An IEEE Photonics Society Publication

Bidirectional Transmission in an Optical Network on Chip With Bus and Ring Topologies

Volume 8, Number 1, February 2016

S. Faralli
F. Gambini, Student Member, IEEE
P. Pintus, Member, IEEE
M. Scaffardi
O. Liboiron-Ladouceur, Senior Member, IEEE
Y. Xiong
P. Castoldi, Senior Member, IEEE
F. Di Pasquale
N. Andriolli
I. Cerutti

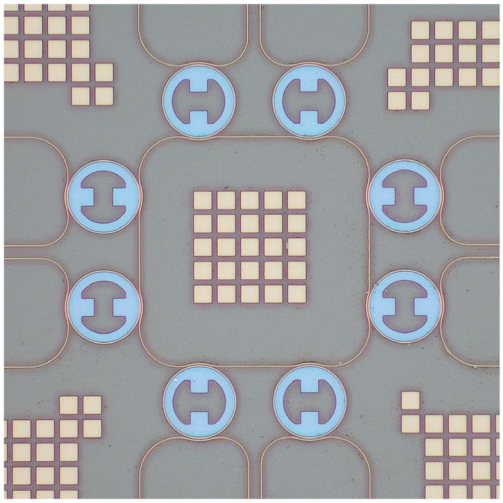

DOI: 10.1109/JPHOT.2016.2526607
1943-0655 © 2016 IEEE

Bidirectional Transmission in an Optical Network on Chip With Bus and Ring Topologies

S. Faralli,[1] F. Gambini,[1,2] *Student Member, IEEE*, P. Pintus,[1,2] *Member, IEEE*, M. Scaffardi,[2] O. Liboiron-Ladouceur,[3] *Senior Member, IEEE*, Y. Xiong,[3] P. Castoldi,[1] *Senior Member, IEEE*, F. Di Pasquale,[1] N. Andriolli,[1] and I. Cerutti[1]

[1]Scuola Superiore Sant'Anna, 56100 Pisa, Italy
[2]Consorzio Nazionale Interuniversitario per le Telecomunicazioni (CNIT), 56124 Pisa, Italy
[3]McGill University, Montreal, QC H3A 0G4, Canada

DOI: 10.1109/JPHOT.2016.2526607

Manuscript received January 29, 2016; accepted February 2, 2016. Date of publication February 8, 2016; date of current version April 15, 2016. This work was supported by the Ministry for Interuniversity Research through FIRB project MINOS, by the Ministero degli Affari Esteri - Unità per la cooperazione Scientifica e Tecnologica (Italian Ministry of Foreign Affair - Unit for Scientific and Technological Cooperation) through bilateral project NANO-RODIN, and by the European Commission through FP7 project IRIS (619194). The authors acknowledge CMC Microsystems for the foundry service. Corresponding author: S. Faralli (e-mail: s.faralli@sssup.it).

Abstract: In photonic integrated networks on chip (NoCs), microrings are commonly used for adding or dropping a single optical signal to be switched in the NoC. This paper demonstrates the feasibility of adding or dropping two optical signals at the same wavelength in the same microring of NoCs with bus and ring topology. More specifically, the same microring can be used to support simultaneous bidirectional transmissions of two signals to be coupled in the NoC topology, leading to two different configurations, called shared source-microring and shared destination-microring. Spectral characterization shows good agreement between simulations and measurements taken on silicon-based integrated NoC. Bit-error-rate (BER) measurements indicate that the shared source-microring configuration performs better, achieving a penalty as low as 1.5 dB for a BER of 10^{-9} at 10 Gb/s in the bus NoC. A higher penalty in the ring NoC for both configurations is due to higher crosstalk in the interconnecting ring.

Index Terms: Silicon nanophotonics, integrated photonic systems, optical interconnect.

1. Introduction

In modern multi-core computing systems, the exchange of data between processors requires fast electronic networks on chip (NoC). Various NoC topologies are used, ranging from bus, to ring, and to more complex multi-stage topologies, trading complexity for scalability and latency.

Over the past few years, photonic integrated NoC have been proposed and investigated [1]–[5], with the aim of demonstrating the feasibility and advantages of optics in overcoming the limitations of electronic NoCs. Photonic integrated circuits (PIC) of NoC enable the exchange of data using optical signals that are generated at the NoC ports and coupled into the NoC topology (e.g., bus, ring, and crossbar). Coupling of the optical signal is often achieved by exploiting

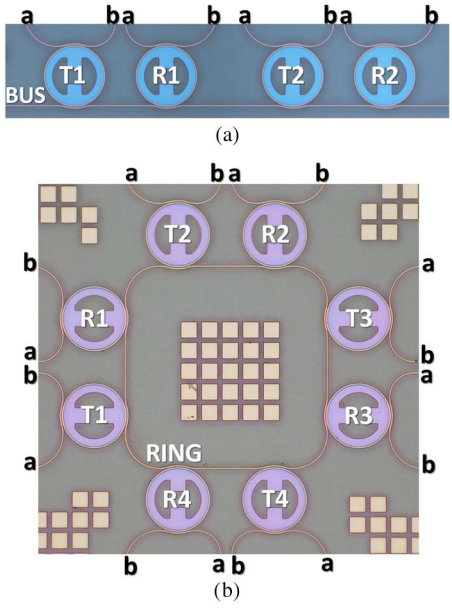

Fig. 1. Photonic integrated circuits implementing the NoCs. (a) Bus NoC. (b) Ring NoC.

the add/drop behavior of resonating microrings. So far, tunable microrings have been typically exploited in NoCs for adding or dropping a single optical signal at a given resonating wavelength or, eventually, a comb of optical signals at different resonating wavelengths (i.e., separated by multiple of free-spectral range). For instance, coupling through microrings was used in integrated optical PICs of the NoCs using bus and ring topologies [5]. A good performance in terms of bit error rate (BER) was achieved in those PICs when transmitting a single optical signal or two optical signals at the same wavelength between distinct pairs of I/O ports co-propagating in the topology [5].

The possibility to support only a single transmission or multiple co-propagating transmissions in a NoC on a given wavelength can be a limitation for some topologies and when high throughput is required. For instance, for bus topologies, an additional counter-propagating bus is needed, which may require thus a larger footprint and several waveguide crossings. Few previous works overcome this limitation by considering bidirectional optical transmissions using either a different wavelength for each direction or non-reciprocal microrings [6]. A first spectral characterization of a bidirectional filter bank realized with a cascade of two microrings is presented in [7].

This paper proposes and assesses the use of bidirectional transmissions in NoCs with bus and ring topology, which were previously tested with unidirectional transmissions only [8]. Even though the cited NoCs can support WDM transmissions, this paper focuses on their performance when simultaneous counter-propagating transmissions occur on the same wavelength and are coupled from or to the same microring. System-level performance are measured for two data patterns at 10 Gb/s generated and optically transmitted on PICs realized with Silicon-on-Insulator (SOI) technology. Injection or removal of the two optical signals occurs at same coupling microring, leading to two configurations: shared source-microring and shared destination-microring. System characterization identifies the best performing configurations and topologies, indicating the feasibility of the approach. To the best of the authors' knowledge, this is the first time that bidirectional data transmissions are tested in PIC NoCs, paving the way for exploitation of bidirectional transmission in other similar PIC designs and topologies.

2. Photonic Integrated NoC Architecture and Design

The considered photonic integrated NoCs are realized with either bus or ring topologies as shown in Fig. 1(a) and (b), respectively. They enable the bidirectional communication between

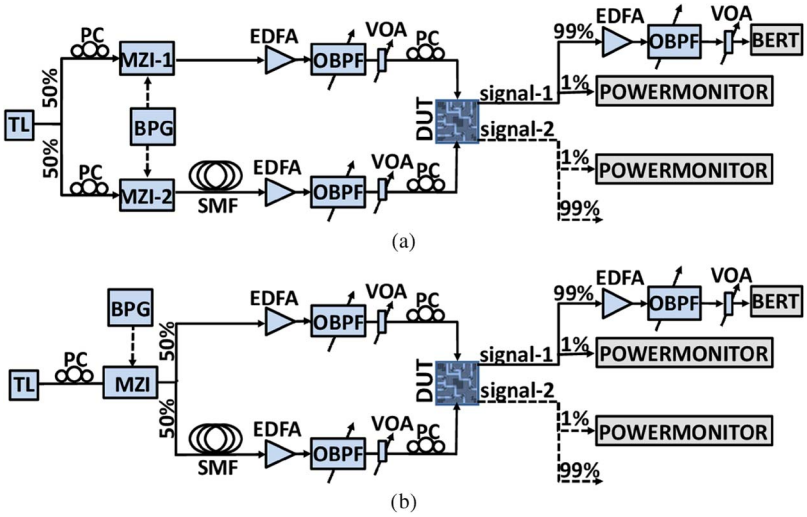

Fig. 2. Diagram of the experimental setup. (a) Bus NoC. (b) Ring NoC.

multiple tiles on a single chip (e.g., CPUs or shared memories). Each NoC is fabricated in silicon photonics and consists of microring-based switching elements, acting either as transmitters or as receivers (labeled as *Ti* or *Rj*, $1 \leq i, j \leq 4$, respectively). Each transmitter (receiver) microring has two ingress (egress) ports, labeled *a* and *b* in the figure, enabling bidirectional data transmission (reception). In addition, each microring is connected to neighboring microrings in a bus or ring topology by means of two other ports.

Each ingress (egress) port is connected to the transmitters (receivers), which are to be linked to CPUs or shared memory. In this silicon photonic demonstration, each transmitter (receiver) consists of an off-chip laser source and modulator (an off-chip photoreceiver). Wavelength selectivity to perform add and drop operations is enabled by thermally tuning the microrings at the intended ingress and egress ports, respectively.

The silicon photonic PICs were fabricated through CMC Microsystems by the Institute of Microelectronics (IME) on 220-nm SOI wafers. Fabricated PICs are displayed in Fig. 1. The waveguides support single-mode TE transmission. The ring NoC consists of the local microrings that add (drop) the optical signals from (to) the input (output) ports and a central microring that connects all the ports, realizing the ring topology. The local microrings have a radius of 10 μm and are designed to achieve a coupling coefficient of 10% in each coupler. The propagation loss of the fabricated silicon waveguides is 2 dB/cm, while the bending loss for a bending radius larger than 5 μm are estimated negligible. In the ring NoC topology, the length of the central ring has been set so that the ratio between the free spectral range of each microring and of the central ring is four [8], [9].

Single-polarization grating couplers are connected to the termination ports enabling the optical I/O to and from the PIC. To tune the microring resonances, each microring switching element is thermally controlled using coplanar n-doped resistive silicon heaters inside each microring [5]. Additional design details of the fabricated PIC are available at [9].

3. Testbed for Bidirectional Transmission

System-level testing of bidirectional transmissions in the microring is carried out using the setups shown in Fig. 2.

For the bus PIC, the experimental setup is shown in Fig. 2(a). An optical signal at about 1550 nm with an optical power of 10 dBm is generated by an external cavity tunable laser (TL). The linewidth is set to 100 MHz by activating the coherence control that helps to reduce the impact of possible residual coherent crosstalk. This signal is split into two arms by a 3-dB optical splitter. In each arm, the signal is modulated by a Mach–Zehnder Interferometer (MZI) fed by a

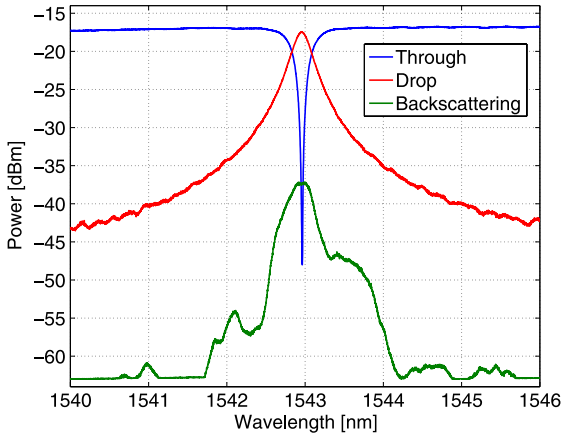

Fig. 3. Spectra of the through, dropped, and backscattered signal in a single microring test structure.

$2^{31} - 1$ pseudo random binary sequence at 10 Gb/s with a bit pattern generator (BPG). A 50 m single mode fiber (SMF) spool is inserted in one arm (the lower arm in the figure) to decorrelate the bit streams of the two signals. Each signal is then amplified by two different erbium doped fiber amplifier (EDFA), filtered by an optical band pass filter (OBPF) and then power-controlled using a variable optical attenuator (VOA). Two polarization controllers (PC) are then used to maximize the optical coupling of each signal into the device under test (DUT). The maximum input signal power coupled to the grating coupler is 16 dBm. Since the coupling loss of the fabricated grating coupler is about 5 dB, the optical power coupled to the silicon waveguide is well below the non-linear power threshold [10]. An eight-port fiber array is used to couple light into up to eight grating couplers of the DUT. A six-pin electrical DC probe is used to independently tune each microring. At the receiver side, one of the signals (see signal-1 in Fig. 2) exiting from the DUT is amplified by an EDFA and filtered by an optical band pass filter (OBPF). The optical signal-to-noise ratio is kept constant at 38 dB at the EDFA output and the optical power at the photodetector of the BER tester (BERT) is controlled by a VOA.

For the ring PIC, the experimental setup has been later replicated with minor modifications, as shown in Fig. 2(b). The setup in Fig. 2(b) behaves as the one in Fig. 2(a). Since the performance measurements are limited to same-wavelength transmissions, a single laser source and a single modulator are used for both channels, which are then decorrelated with a 1 km SMF spool.

4. Bidirectional Transmission Performance

Before characterizing the NoCs, a single microring (identical to the switching elements in the bus and ring NoCs) is selected as reference and assessed in terms of spectral response. The measurement is taken by injecting the signal at the input port by a tunable laser and measuring the spectra by a power meter at the different output ports: through, drop, and add ports (the latter is called backscattering port). The spectra are shown in Fig. 3. At the resonance frequency, the signal power at the backscattering port is below 20 dB of the dropped signal. In the following subsections, the spectral characterization and the transmission performance of bus and ring photonic integrated NoCs are reported. The free spectral range (FSR) of the local ring resonator is about 9.6 nm, while the one of the central microring is about 2.4 nm.

4.1. Bus NoC

The spectral characterization of the bus PIC is performed and compared with the simulation results. Simulated and measured spectra of the transmission from the port $T1b$ to the port $R1a$ ($T1b \rightarrow R1a$) are reported in Fig. 4 (top and bottom subfigures, respectively). The simulations are obtained using the transfer matrix method [8] and assuming identical and lossless coupling between microrings and waveguides. Simulations are set by tuning the resonance frequency of

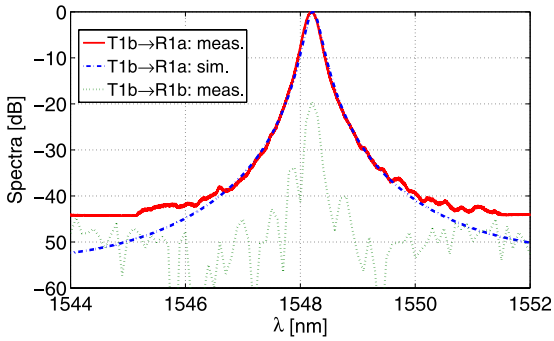

Fig. 4. Simulated (top) and measured (bottom) transmission spectra of the network on chip based on bus topology, including the backscattering noise.

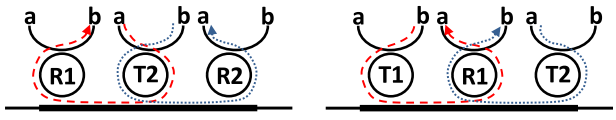

Fig. 5. Tested configurations in the bus and ring NoC. (a) Shared source-microring. (b) Shared destination-microring.

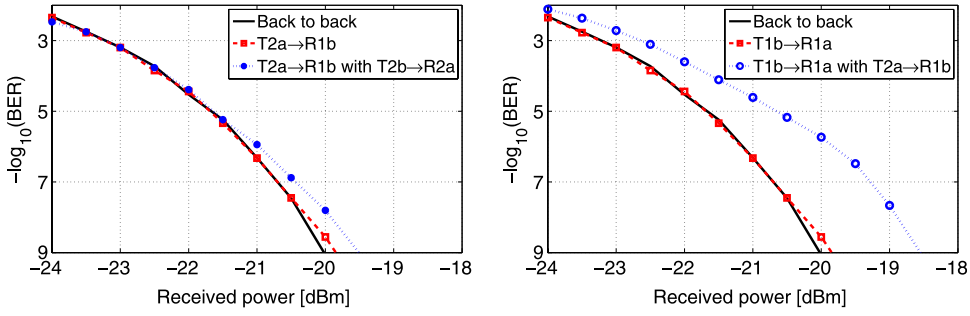

Fig. 6. BER vs. received power at the output port *R*1*b* in the bus topology for two different configurations. (a) Shared source-microring and (b) shared destination-microring.

the microrings at the same operating wavelength (i.e., 1548.21 nm) and the results predict the measured spectra with good accuracy, as shown in Fig. 4. The simulated and measured 3-dB bandwidths are, respectively, 25.5 GHz and 27.88 GHz, and the discrepancy between the simulated and measured values can be mainly ascribed to the fabrication tolerances. Experimental results of backscattering noise ($T1b \rightarrow R1b$) show a crosstalk below –20 dB.

Fig. 6 shows the bit error rate (BER) as a function of the received power for the transmission of two distinct 10 Gb/s data streams at the same operating wavelength of 1548.21 nm in two different tested configurations: shared source-microring and shared destination-microring as shown in Fig. 5(a) and (b), respectively.

In the shared source-microring configuration, the two modulated optical signals are injected from the two input ports *a* and *b* of the same microring (e.g., *T*2) and are routed to an upstream output port and a downstream output port, i.e., on distinct destination microrings (e.g., *R*1 and *R*2). Fig. 6(a) shows the BER measured at port *R*1*b* with and without the simultaneous transmission $T2b \rightarrow R2a$. The BER of the transmission $T2a \rightarrow R1b$ outperforms the back-to-back BER for low error rates, thanks to the filtering effects of the microrings [4], [5]. The corresponding eye diagrams are reported in Fig. 7: (a) Back-to-back and (b) shared source-microring. When the simultaneous transmission $T2b \rightarrow R2a$ at the same wavelength is added, the BER degradation is 0.5 dB at a BER of 10^{-9}.

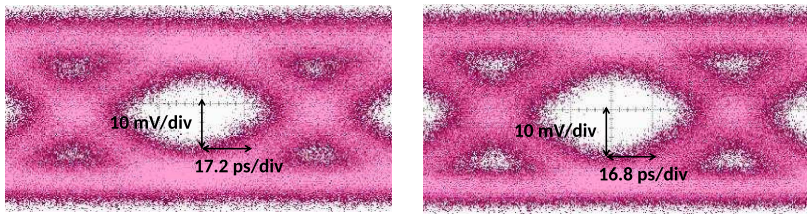

Fig. 7. Eye diagrams for shared source microring. (a) Back-to-back. (b) $T1a \rightarrow R2b$.

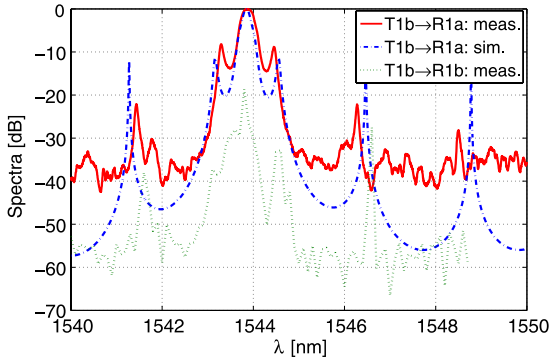

Fig. 8. Simulated (top) and measured (bottom) spectra of the network on chip based on ring topology, including the backscattering noise.

In the shared destination-microring configuration, the two modulated optical signals are injected from two input ports of two distinct microrings (e.g., port $T1$ and port $T2$) and are directed to the two output ports a and b of the same destination microring (e.g., $R1$). Fig. 6(b) shows a comparison of the BER values measured at port $R1a$ with and without the simultaneous transmission $T2a \rightarrow R1b$. In the presence of the transmission $T2a \rightarrow R1b$ at the same wavelength, the BER degradation is approximately 1.5 dB at a BER of 10^{-9}, which is higher than in the shared source-microring configuration. Indeed, a stronger signal crosstalk at the receivers $R1a$ and $R1b$ is caused by the backscattering at the destination microring and by the reflections induced by the grating couplers of the two incoming counter-propagating signals.

4.2. Ring NoC

The spectral characterization of the ring PIC is performed and compared with the simulated results for the transmission from the port $T1b$ to the port $R1a$ ($T1b \rightarrow R1a$). As for the bus PIC, the simulated results are calculated using the transfer matrix method [8]. The spectral responses are obtained by tuning the resonance frequency of the microrings at the same operating wavelength of 1543.86 nm. Fig. 8 confirms the good agreement between measured and simulated spectra. The primary peaks are due to the resonance frequency of the microrings, whereas the secondary peaks are generated by the central ring when resonating. The simulated and measured 3-dB bandwidths are, respectively, 28.7 GHz and 22.2 GHz. Experimental results of backscattering noise ($T1b \rightarrow R1b$) show a crosstalk below −19 dB.

The transmission performance for the two configurations are reported in Fig. 9. The BER slightly deteriorates in the ring topology compared to the bus topology, for both transmission configurations. The degradation is caused by the presence of the central ring that acts as a recirculation loop. In the shared source-microring configuration, the penalty of the bidirectional transmission is limited to 2.5 dB for a BER of 10^{-9}. In shared destination-microring configuration, the transmission penalty is higher than in the shared-source configuration due to reflections and backscattering close to receivers and reaches 4.5 dB for a BER of 10^{-9}.

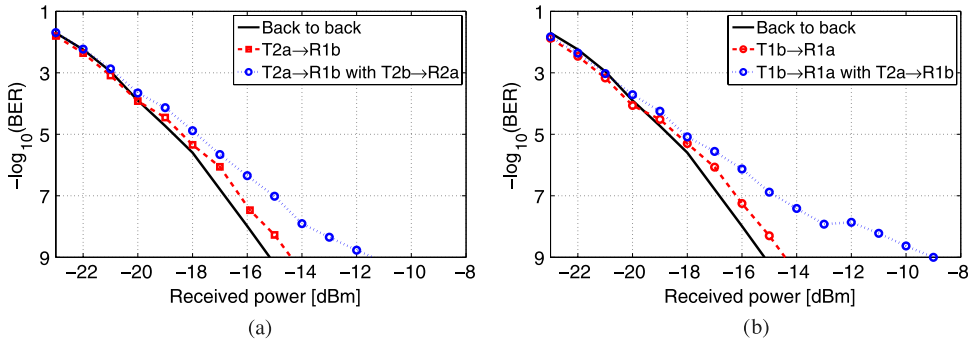

Fig. 9. BER vs. received power at the output port *R*1*b* and *R*1*a* in the ring topology for two different configurations. (a) Shared source-microring and (b) shared destination-microring.

5. Conclusion

The use of microrings for adding and dropping the optical signal in integrated NoC is well established. This paper proposed and experimentally demonstrated for the first time the possibility of bidirectional transmissions at the same wavelength in the add/drop microrings of NoC.

Bidirectional data transmissions were tested on Si-based PICs realizing NoC with either bus or ring topology. The fabricated PIC NoCs achieve a backscattering of 20 dB below the signal, as predicted through simulations. An excellent performance was achieved by the bus PIC with a BER degradation below 1 dB when two different transmissions share the same microring used to couple the signals into the bus (shared source-microring). A slightly higher BER degradation is experienced when sharing the same destination microring (shared destination-microring). The same relative performance between the two configurations holds for the ring PIC, but with higher BER penalty due to the signal recirculation in the central ring causing higher crosstalk.

These experimental achievements indicate the feasibility of bidirectional transmissions, enabling a greater flexibility and opportunity for higher throughput in the NoCs, especially when combined with WDM. Another potential application would be for supporting flow control messages in one of the two directions. All these benefits can find exploitation in other NoC topologies and PIC designs as well.

References

[1] Y. Vlasov, W. M. Green, and F. Xia, "High-throughput silicon nanophotonic wavelength-insensitive switch for on-chip optical networks," *Nature Photon.*, vol. 2, no. 4, pp. 242–246, Mar. 2008.
[2] A. Biberman *et al.,* "Broadband silicon photonic electrooptic switch for photonic interconnection networks," *IEEE Photon. Technol. Lett.*, vol. 23, no. 8, pp. 504–506, Apr. 2011.
[3] L. Chen and Y. Chen, "Compact, low-loss and low-power 8 × 8 broadband silicon optical switch," *Opt. Exp.*, vol. 20, no. 17, pp. 18 977–18 985, Aug. 2012.
[4] A. Parini *et al.,* "BER evaluation of a passive SOI WDM router," *IEEE Photon. Technol. Lett.*, vol. 25, no. 23, pp. 2285–2288, Dec. 2013.
[5] S. Faralli, F. Gambini, P. Pintus, I. Cerutti, and N. Andriolli, "Ring versus bus: A BER comparison of photonic integrated networks-on-chip," in *Proc. IEEE OI*, 2015, pp. 22–23.
[6] D. Dai and J. E. Bowers, "Silicon-based on-chip multiplexing technologies and devices for Peta-bit optical interconnects," *Nanophotonics*, vol. 3, no. 4/5, pp. 283–311, 2014.
[7] M. S. Dahlem *et al.,* "Reconfigurable multi-channel second-order silicon microring-resonator filterbanks for on-chip WDM systems," *Opt. Exp.*, vol. 19, no. 1, pp. 306–316, Jan. 2011.
[8] P. Pintus *et al.,* "Ring versus bus: A theoretical and experimental comparison of photonic integrated NoC," *J. Lightw. Technol.*, vol. 33, no. 23, pp. 4870–4877, Dec. 2015.
[9] P. Pintus, P. Contu, P. G. Raponi, I. Cerutti, and N. Andriolli, "Silicon-based all-optical multi microring network-on-chip," *Opt. Lett.*, vol. 39, no. 4, pp. 797–800, Feb. 2014.
[10] E. Dulkeith, Y. A. Vlasov, X. Chen, N. C. Panoiu, and R. M. Osgood, "Self-phase-modulation in submicron silicon-on-insulator photonic wires," *Opt. Exp.*, vol. 14, no. 12, pp. 5524–5534, Jun. 2006.